Title	The structural changes in crystalline cellulose and effects on enzymatic digestibility
Author(s)	Horikawa, Yoshiki; Konakahara, Naoya; Imai, Tomoya; Kentaro, Abe; Kobayashi, Yoshinori; Sugiyama, Junji
Citation	Polymer Degradation and Stability (2013), 98(11): 2351-2356
Issue Date	2013-11
URL	http://hdl.handle.net/2433/179455
Right	© 2013 Elsevier Ltd.
Type	Journal Article
Textversion	author

The structural changes in crystalline cellulose and effects on enzymatic digestibility

Yoshiki Horikawa[1], Naoya Konakahara[1], Tomoya Imai[1], Abe Kentaro[1], Yoshinori Kobayashi[2], Junji Sugiyama[1]

[1]Research Institute for Sustainable Humanosphere, Kyoto University, Kyoto, Japan

[2]Tsukuba Research Laboratory, Japan Bioindustry Association, Ibaragi, Japan

Correspondence to: Yoshiki Horikawa, Research Institute for Sustainable Humanosphere, Kyoto University, Uji, Kyoto 611-0011, Japan.

E-mail: yhorikawa@rish.kyoto-u.ac.jp

Tel: +81-774-38-3634; Fax: +81-774-38-3635

Abstract

The enzymatic hydrolysis of cellulose I achieves almost complete digestion when sufficient enzyme loading as much as 20mg/g-substrate is applied. However, the yield of digestion reaches the limit when the enzyme dosage is decreased to 2mg/g-substrate. Therefore, we have performed three pretreatment such as mercerization, dissolution into phosphoric acid and EDA treatment. Transformation into cellulose II hydrate by mercerization and dissolution into phosphoric acid were not sufficient because substrate changed to highly crystalline structure during saccharification. On the other hand, in the case of crystalline conversion of cellulose I to III_I by EDA, almost perfect digestion was achieved even in enzyme loading as small as 0.5 mg/g-substrate, furthermore, hydrolyzed residue was typical cellulose I. The structural analysis of substrate after sacchafication provides an insight into relationships between cellulose crystalline property and cellulase toward better enzymatic digestion.

Keywords:

Crystalline polymorph, enzymatic hydrolysis, susceptibility, FTIR spectroscopy

Introduction

The excessive consumption of fossil resources induces the shortage of energy and the serious problem of global warming, which have prompted the research and development of alternative energy sources from renewable substance. Lignocellulosic biomass is a hopeful material because of non-competition with food and it includes large amount of cellulose which is fermentable sugars (Himmel et al. 2007; Jørgensen et al. 2007). However, Cellulose is an insoluble crystalline polymer, which decreases the enzymatic conversion from lignocellulose to monosaccharide. The efficient pretreatment, therefore, is required to enhance the susceptibility of cellulose by removing the matrix component as well as modification of cellulose structural property, which conducts the reduction of enzyme dosage.

The natural cellulose is composed of two crystalline allomorphs, namely I_α and I_β (Atalla and Vanderhart, 1984), which has been determined crystallographic units as one-chain triclinic and two-chain monoclinic unit cells, respectively (Sugiyama et al. 1991). Further precise structure including hydrogen bonding network has been characterized by synchrotron X-ray and neutron diffraction analysis (Nishiyama et al., 2002, 2003). The digestibility of cellulose polymorph has been reported that I_α-rich cellulose produced by acetobacter or marine algae is higher susceptible than I_β cellulose (Hayashi et al. 1998a b). Igarashi et al. (2007) found the transformation of cellulose I into cellulose III_I is an outstanding effect for enzymatic hydrolysis. They also reported little difference in digestibility between cellulose I_α and I_β by using crystalline transition technique (Yamamoto et al. 1989). Wada et al. (2010) demonstrated the mercerization, which convert from cellulose I to cellulose II, has great potential for better saccharification. These works are motivated to investigate the effect on crystalline structure for efficient ethanol production (Mittal et al. 2011; Ciolacu et al. 2011; Ioelovich and Morag, 2011), however, the use of cellulose from various origins make difficult to fairly assess the enzymatic digestibility. In addition, as a crystalline substrate for enzymatic degradation, microcrystalline cellulose standards such as Avicel and Whatman cellulose have been employed. However, these materials are practically different from cellulose microfibrils in the lignocellulosic biomass.

In this report, therefore, well-dispersed microfibriller cellulose was prepared from *Eucalyptus globules* by mechanical grinding and use as starting substrate. Moreover, cellulose crystalline polymorphs and phosphoric acid-swollen cellulose as a non-crystalline substrate are prepared, and then, all of which compared the susceptibility to cellulase. Furthermore, the characterization of residue after

saccharification will be described for better understanding why enzymatic inhibition was occurred.

Material and method

Sample preparation

The highly dispersed cellulose I was prepared according to the protocol reported by Abe et al. (2006). *E. globulus* wood chips given from Oji Paper Co., Ltd. (Tokyo Japan) were processed in two stage milling: The first was roughly milled by Orient mill VM-16 (Seishin Enterprise Corp., Tokyo, Japan) and the second was subjected to pass a 150-μm screen by Bantam mill AP-BL (Hosokawa micron Corp., Osaka, Japan). The products were treated in acidified sodium chlorite solution at 70 °C for in removal of lignin (Wise et al. 1946). This process was repeated until an infrared band at 1510 and 1600 cm^{-1}, which were ascribed to the aromatic skeletal vibration, disappeared completely. Following this, the samples were boiled in 5% NaOH for several hours. The band at 1370 cm^{-1} characteristic of xylan was monitored to disappear in the FTIR spectra from processed sample. Finally, purified pulp was passed through a grinder (Masuko Corp.) at 1500 rpm (Taniguchi and Okamura 1998; Iwamoto et al. 2005). The sample was condensed by centrifugation at 5,000 g for following enzymatic hydrolysis.

The cellulose II hydrate was prepared to immerse the grinder passed cellulose I in 20 % NaOH solution. The crystalline transformation was performed by gently stirring at room temperature for 1h and then washed in distilled water several time until neutrality.

The conversion of cellulose III_I was performed by soaking the highly dispersed cellulose I in aqueous ethylenediamine (EDA) solvent (Roche and Chanzy 1981). After swelling in a 75 : 25 mixture of EDA and H_2O at room temperature, the samples were washed in methanol for 10min. The whole process was repeated until the band at 3445 cm^{-1}, which is assigned to O3H-O5 of cellulose I, disappeared. The converted samples were washed in distilled water several times for following enzymatic saccharification.

Phosphoric acid-swollen cellulose (PASC) was prepared by immersed corresponding cellulose I in 85 % phosphoric acid and gently stirred for 1h on ice. Regenerated cellulose was precipitated by an addition of cold water followed by washed in distilled water for several time.

Enzymatic hydrolysis

The enzyme employed for saccharification was a commercial cocktail Accellerase 1500 (Genencor, Danisco US, Inc. Rochester, NY). The enzymatic hydrolysis were performed with 20 mg of cellulose substrate in 2 ml of 100 mM acetate buffer (pH 5.0) containing the enzyme at 20, 2, 1 and 0.5 mg/g-substrate (corresponding to 32, 3.2, 1.6 and 0.8 FPU (the filter paper activity)), respectively. FPU was measured along the standard protocol recommended by NREL (2010). The mixtures were incubated at 50˚C with 150 strokes / min for 144 h, and the glucose liberated was analyzed by using D-glucose assay kit (Roche Co. Ltd.).

Transmission Electron Microscopy

Cellulose suspension was spotted on a micro-grid (purchased from Okenshoji Co., Ltd.) and then rapid-freezed into liquid ethan in a Reichert KF80 quick-freezing unit (Leica). The grid with keeping the ultracold condition was inserted in and observed by employing a JEM-2000EXII transmission electron microscope (Jeol Co. Ltd.) operated at 100 kV at low temperature around -190 ºC in a Gatan cryo-holder.

X-ray diffractometry

Disk sample prepared from each freeze-dried material and then molding with a handpress. X-ray diffractometry was performed in the reflection mode employing Cu-Kα radiation generated from UltraX 18HF (Rigaku Co. Ltd.) operating at 30 kV and 100 mA ($\lambda = 0.1542$ Å).

FTIR spectroscopy

FTIR Spectra were recorded on a Perkin Elmer SPECTRUM ONE FTIR spectrometer equipped with an AUTO IMAGE microscope accessory ranging from 4000 to 700 cm^{-1}. The spectra were given with a low noise detector (HgCdTe) that was cooled at –196 °C with a spectral resolution of 4 cm^{-1} and acquisition of 128 scans. Cellulose suspension was dropped on the BaF_2 window (13 mm diameter × 2 mm thickness) and dried completely for spectral acquisition.

PCA (Principal Component Analysis)

PCA was performed by using commercial software (Unscrambler v.9.8; CAMO Software, Inc., Woodbridge, NJ) based on the FTIR spectra recorded from residue of cellulose III_I hydrolyzed at 1mg/g-substrate for 0, 6, 12, 24, 48, 72 and 144 h.

Result and discussion

Preparation of standard cellulose I, II, III_I and PASC as a substrate for enzymatic hydrolysis

In order to prepare suitable substrate from lignocellulosic biomass for enzymatic hydrolysis, cellulose samples after removal of lignin and hemicellulose from *E. globulus* wood powder was passed through a grinder. The slurry obtained showed higher viscosity and typical wood cells of hardwood such as tracheary element and xylem fiber have never been visible under optical microscopy. Negative staining technique with uranyl acetate for TEM experiment gives higher resolution, but sometime induces an artificial aggregation of cellulose fibers during drying up the specimen on the grid. Therefore, cryo-TEM observation was performed on grinder passed cellulose I that embedded in vitrified ice by rapid freezing. Figure 1a shows micrograph of cellulose fibers which was highly dispersed and maintained long length different from avicel that occurred in levelling-off degree of polymerization by severe chemical treatment. This is the standard sample as cellulose I that we used to prepare following cellulose II hydrate, III_I and PASC.

Figure 2 exhibits the X-ray diffractograms of highly dispersed cellulose I and cellulose samples after crystalline transformation or dissolution in phosphoric acid. The diffractogram of Cellulose II shows typical three peaks at 12.2˚, 20.8˚ and 21.4˚, corresponding to $(1\,\bar{1}\,0)_{II}$, $(110)_{II}$ and $(200)_{II}$, respectively. The transformation from cellulose I to cellulose III_I can be seen in the peak shift of (200) from the value at 22.4 to 21.0, and appearance of a peaks ascribed to $(1\,\bar{1}\,0)_{III_I}$ and $(002)_{III_I}$. The EDA technique is different from the treatment with liquid ammonia in that a repeat of swelling and deswelling washed in methanol might cause lattice distortion of cellulose microfibril, which resulting in the less peak of $(1\,\bar{1}\,0)_{III_I}$ and $(002)_{III_I}$. To confirm if fiber morphology was maintained or not, cellulose sample after EDA treatment was observed with cryo-TEM technique. The TEM micrograph showed the long chains as well as before corresponding treatment (Figure 1b), which indicated transformation with EDA processing increase distortion of cellulose molecules, but keep the microfibril morphology. Almost complete conversion of cellulose I into cellulose II or cellulose III_I can be observed by disappearance of peaks at 14.6˚ and 16.4˚ characteristic of $(110)_I$ and $(1\,\bar{1}\,0)_I$, respectively.

PASC was constructed of disorganized cellulose molecules, therefore, wholly showed broad curve without shaper peaks (Figure 1d). It is well known that the small crystalline size and disordered molecules provided broad peak in X-ray diffractogram.

Effect of susceptibility on cellulose crystalline morphology

Enzymatic hydrolysis of different polymorphic forms from Eucalyptus cellulose was carried out by commercial cellulase, named as Accellerase 1500, loading at 20, 2, 1 and 0.5 mg/g-substrate (Figure 3). For cellulose I, most of the substrate can achieve complete digestion when sufficient enzyme loading as much as 20 mg/g-substrate is applied. The yield of saccharification, however, reaches the limit when the enzyme loading is decreased to 2 mg/g-substrate (Figure 3a). In order to modify this limitation, natural cellulose was converted into cellulose II hydrate. The digestibility was partially improved as the use of cellulase loading at 2 mg/g-substrate can reach final glucose concentration applying at 20 mg/g-substrate. However, when the enzyme concentration decreased to 1mg/g-substrate, the perfect hydrolysis could not be achieved (Figure 3b). On the other hand, the EDA treatment for transformation into cellulose III_I showed best efficient for glucose conversion. There was an achievement of complete digestion even though cellulase dosage reduced to 0.5 mg/g-substrate (Figure 3c). Interestingly, though PASC was used as amorphous cellulose substrate, it could not reach equal to saccharification at sufficient enzyme dosage (Figure 3d) as well as cellulose II hydrate.

Characterization of hydrolyzed residue by FTIR spectroscopy

For understanding why further enzymatic hydrolysis has been inhibited when using lower cellulase loading, hydrolysis residue was characterized by FTIR spectroscopy as presented in Figure 4. For cellulose II, spectral pattern after hydrolysis in the range of 3600 - 3000 cm^{-1} was quite different from that before hydrolysis in that the intensities of cellulose II-specific bands at 3488 and 3445 cm^{-1} (Marrinan and Mann, 1956) were increased. The similar spectral absorbance was obtained from PASC hydrolysis applied at 1mg/g-substrate, where corresponding bands characteristic of cellulose II were clearly visible. It is generally accepted that the sharper bands in OH stretching region indicates larger crystallites and higher ordered molecules. It has been reported in the literature that disordered or amorphous cellulose is hydrolyzed easier compared to crystalline cellulose (Fan et al., 1980; Hall et al., 2010), which suggested the proposal that the degree of cellulose molecular arrangement is a key factor in determining the susceptibility to cellulase. Therefore, these rigid structures formed from cellulose II hydrate and PASC in the process of enzymatic hydrolysis, seem to suppress more glucose conversion. Surprisingly, there was typical cellulose I in IR spectrum, where generating apparent band at 3345 cm^{-1} ascribed to O-3-H···O-5 (Márechal and

Chanzy, 2000), after cellulase hydrolysis of cellulose III_I whose spectral feature is a sharp band at 3481 cm^{-1} (Wada et al. 2004). Both of digestion products from cellulose I and III_I after hydrolysis have shorter length compared to that before hydrolysis (Figure 5), especially the residue from cellulose III_I seemed to be small size which might be attributed to more susceptible structure compared to cellulose I. The transformation of cellulose I into cellulose III_I has been known as reversible reaction, and then we performed control experiment where the cellulose III_I is incubated under corresponding condition without cellulase dosage. The spectral pattern of substrate before and after incubation was not different (data not shown), which indicated the crystalline change from cellulose III_I to cellulose I is independent of hydrolyzed temperature of 50 ºC and agitation by shaking the reaction bottle. At least two possibilities can be envisaged for interpreting the generation of cellulose I. One is insufficient initial conversion from cellulose I to III_I, and the other is reconversion from III_I to I caused by the interaction with enzymes. However, there is no direct evidence to conclude from this study. As the structure and origin of this inaccessible cellulose I seems important to understand the saccharification mechanism, the work along this line is in progress.

PCA for digestion product from cellulose III_I

In order to verify the process of crystalline change from cellulose III_I to I during hydrolysis, PCA has been conducted on the IR spectra from residue hydrolyzed by 1mg/g-substrate dosage (Figure 6a). As presented in Figure 6b, the PC1 loading spectra ranging from 3600-3000 cm^{-1} exhibited one negative band at 3481 cm^{-1} and two positive bands at 3345 and 3270 cm^{-1} which is specific to cellulose I_β (Sugiyama et al. 1991). Therefore, the larger amount of cellulose III_I should shift to lower scores for PC1, and the converse direction along PC1 implied the increase of cellulose I ratio. PC2 showed significant positive band at 3481 cm^{-1} , which indicate higher crystalline cellulose III_I shift to higher scores for PC2. The score plots and loading factors demonstrated the course of enzymatic degradation of cellulose III_I as follows; the cellulase initially hydrolyzed the disordered region, and then higher crystalline cellulose III_I were remained. Secondary, cellulose III_I was preferentially-degraded, which resulted in cellulose I was left. Igarashi et al. (2007) discussed this difference of digestibility is due to packing density and distance of hydrophobic surface. Furthermore, same authors recently reported by using high-speed atomic force microscopy that physical property such as area and flatness of crystalline surface where cellobiohydrolase I interacted, is also important for the digestibility (Igarashi et al. 2011). As shown in Figure 3a and 4a, glucose conversion from cellulose I reached a limit when cellulase dosage is decreased,

which might be conducted by the presence of hemicelluloses that tightly associated with cellulose microfibril and then hinder cellulase accessible (Penttilä et al. 2013). However, the evidence obtained from structural analysis for hydrolysis of cellulose III_I clearly demonstrated cellulose I is more recalcitrant substrate compared to cellulose III_I.

Conclusion

The structural analysis after sacchafication provides an insight into relationships between cellulose crystalline property and cellulase toward better enzymatic digestion. Complete digestion has been achieved by EDA pretreatment, where crystalline transformation of cellulose I into cellulose III_I took place as well as cellulose molecular arrangement was disordered, even though enzyme loading decreased to 0.5 mg/g-substrate of commercial cellulase. The change of crystalline structure in the process of hydrolysis was clearly demonstrated cellulose III_I is more susceptibility to cellulase than natural cellulose. On the other hand, cellulose II and dissolution into phosphoric acid could not overcome this limit because cellulose crystallinity was increased during enzymatic hydrolysis. Change of cellulose crystalline structure depending crystalline polymorph was important in determining the digestibility to cellulase.

Acknowledgments

The authors express their appreciation to Ms. K. Kanai and Ms. M. Imai for her technical support on the research. This study was supported by the New Energy and Industrial Technology Development Organization (NEDO).

Figure legends:

Figure 1.

Vitreous-ice-embedding cryo-TEM micrographs of cellulose microfibril extracted from *E.globulus* (a) before and (b) after transformation into cellulose III_I by EDA treatment.

Figure 2

X-ray diffractograms of cellulose (a) I, (b) II, (c) III_I and (d) PASC.

Figure 3

Enzymatic hydrolysis of cellulose (a) I, (b) II, (c) III_I and (d) PASC when cellulase loading at 20, 2 1 and 0.5 mg/g-substrate is applied. Error bars indicate the standard deviation between two measurements.

Figure 4

FTIR spectra of cellulose (a) I, (b) II, (c) III_I and (d) PASC before (bold line) and after enzymatic hydrolysis at 1 mg/g-substrate dosage for 144h (hair line). The bands at 3345 and 3481 cm^{-1} are ascribed to O-3-H···O-5 of cellulose I and III_I, respectively. The bands at 3488 and 3445 cm^{-1} are specific to cellulose II in the OH-stretching region.

Figure 5

Cryo-TEM micrographs of hydrolyzed residue from cellulose I (a) and cellulose III_I (b) for 144h when enzyme loading at 1mg/g-substrate was applied.

Figure 6

(a) PCA score plotted on the first and second principal components of FTIR spectra from hydrolyzed residue of cellulose III_I applied cellulase at 1mg/g-substrate. (b) PC1 (red line) and PC2 loading (blue line) spectrum in the region of 3600-3000 cm^{-1}. The band at 3481 cm^{-1} is specific of cellulose III_I, whereas two bands at 3445 and 3470 cm^{-1} are characteristic of cellulose I.

References

Himmel ME, Ding SY, Johnson DK, Adney WS, Nimlos MR, Brady JW, Foust TD: Biomass recalcitrance: engineering plants and enzymes for biofuels. Science 2007; 315: 804–807

Jørgensen H, Kristensen JB, Felby C: Enzymatic conversion of lignocellulose into fermentable sugars: challenges and opportunities. Biofuels Bioprod Biorefin 2007; 1: 119–134

Atalla RH, VanderHart DL Native cellulose: A composite of two distinct crystalline forms. Science 1984; 223: 283–285.

Sugiyama J, Vuong R, Chanzy H: An electron diffraction study on the two crystalline phases occurring in native cellulose from algal cell wall. Macromolecules 1991; 24: 4168–4175.

Nishiyama Y, Langan P, Chanzy H: Crystal structure and hydrogen-bonding system in cellulose I_β from synchrotron X-ray and neutron fiber diffraction. J Am Chem Soc 2002; 124: 9074–9082.

Nishiyama Y, Sugiyama J, Chanzy H, Langan P: Crystal structure and hydrogen bonding system in cellulose I_α from synchrotron X-ray and neutron fiber diffraction. J Am Chem Soc 2003;125: 14300–14306.

Hayashi N, Sugiyama J, Okano T, Ishihara M: Selective degradation of the cellulose I_α component in *Cladophora* cellulose with *Trichoderma viride* cellulase. Carbohydr Res 1998; 305: 109-116.

Hayashi N, Sugiyama J, Okano T, Ishihara M: The enzymatic susceptibility of cellulose microfibrils of the algal-bacterial type and the cotton-ramie type. Carbohydr Res 1998; 305: 261-269.

Igarashi k, Wada M, Samejima M: Activation of crystalline cellulose to cellulose III_I results in efficient hydrolysis by cellobiohydrolase. FEBS J 2007; 274: 1785–1792.

Yamamoto H, Horii F, Odani H: Transformation of *Valonia* cellulose crystals by an alkaline hydrothermal treatment. Macromolecules 1990; 23: 3196-3198.

Wada M, Ike M, Tokuyasu K: Enzymatic hydrolysis of cellulose I is greatly accelerated via its conversion to the cellulose II hydrate form. Polym Degrad Stab 2010; 95: 543–548.

Ioelovich M, Morag E: Effect of cellulose structure on enzymatic hydrolysis. BioResources 2011; 6 (3); 2818-2835.

Mittal A, Katahira R, Himmel ME, Johnson1 DK: Effects of alkaline or liquid-ammonia

treatment on crystalline cellulose: changes in crystalline structure and effects on enzymatic digestibility. Biotechnol. Biofuels 2011; 4:41–56.

Ciolacu D, Gorgieva S, Tampu D, Kokol V: Enzymatic hydrolysis of different allomorphic forms of microcrystalline cellulose. Cellulose 2011; 18: 1527–1541.

Abe K, Iwamoto S, Yano H: Obtaining cellulose nanofibers with a uniform width of 15nm from wood. Biomacromolecules 2007; 8: 3276–3278.

Wise LE, Murphy M, D'Addieco A: Chlorite holocellulose, its fractionation and beating on summative wood analysis and studies on the hemicelluloses. Pap Trade J 1946; 122(2): 35−43

Taniguchi T, Okamura K: New films produced from microfibrillated natural fibres. Polym Int 1998; 47: 291−294.

Iwamoto S, Nakagaito AN, Yano H, Nogi M: Optically transparent composites reinforced with networks of bacterial nanofibers. Appl. Phys. A 2005; 81: 1109−1112.

Roche E, Chanzy H: Electron microscopy study of the transformation of cellulose I into cellulose III_I in *Valonia*. Int J Biol Macromol 1981; 3: 201−206

Adney B, Baker J: Measurement of cellulase activities. Technical Report NREL 1996; TP-510-42628.

Marrinan J, Mann J: Infrared spectra of the crystalline modifications of cellulose. J Polym Sci 1956; 21: 301–311.

Fan LT, Lee YH, Beardmore DH: Mechanism of the enzymatic hydrolysis of cellulose: effect of major structural features of cellulose on enzymatic hydrolysis. Biotechnol Bioeng 1980; 23:177−199.

Hall M, Bansal P, Lee JH, Realff MJ, Bommarius AS: Cellulose crystallinity−a key predictor of the enzymatic hydrolysis rate. FEBS J 2010; 277:1571−1582.

Márechal Y. and Chanzy H. 2000. The hydrogen bond network in I-beta cellulose as observed by infrared spectrometry. J. Mol. Struc. 523: 183–196.

Wada M, Heux L, Sugiyama J: Polymorphism of Cellulose I Family: Reinvestigation of Cellulose IV_I. Biomacromolecules 2004; 5: 1385−1391.

Penttilä PA, Várnai A, Pere J, Tammelin T, Salmén L, Siika-aho M, Viikari L, Serimaa R: Xylan as limiting factor in enzymatic hydrolysis of nanocellulose. Bioresour Technol 2013; 129: 135–141

Igarashi K, Uchihashi T, Koivula A, Wada M, Kimura S, Okamoto T, Penttilä M, Ando T, Samejima M: Traffic jams reduce hydrolytic efficiency of cellulase on cellulose surface. Science 2011; 333: 1279–1282.

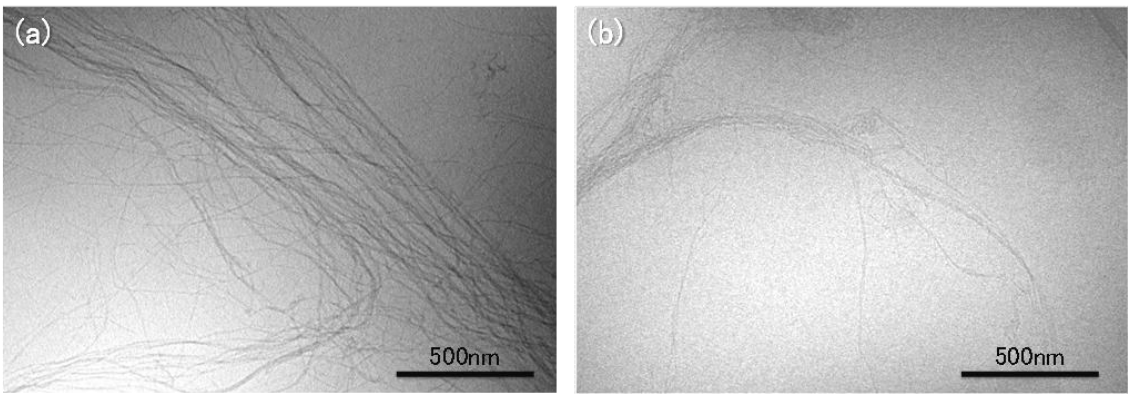

Figure 1

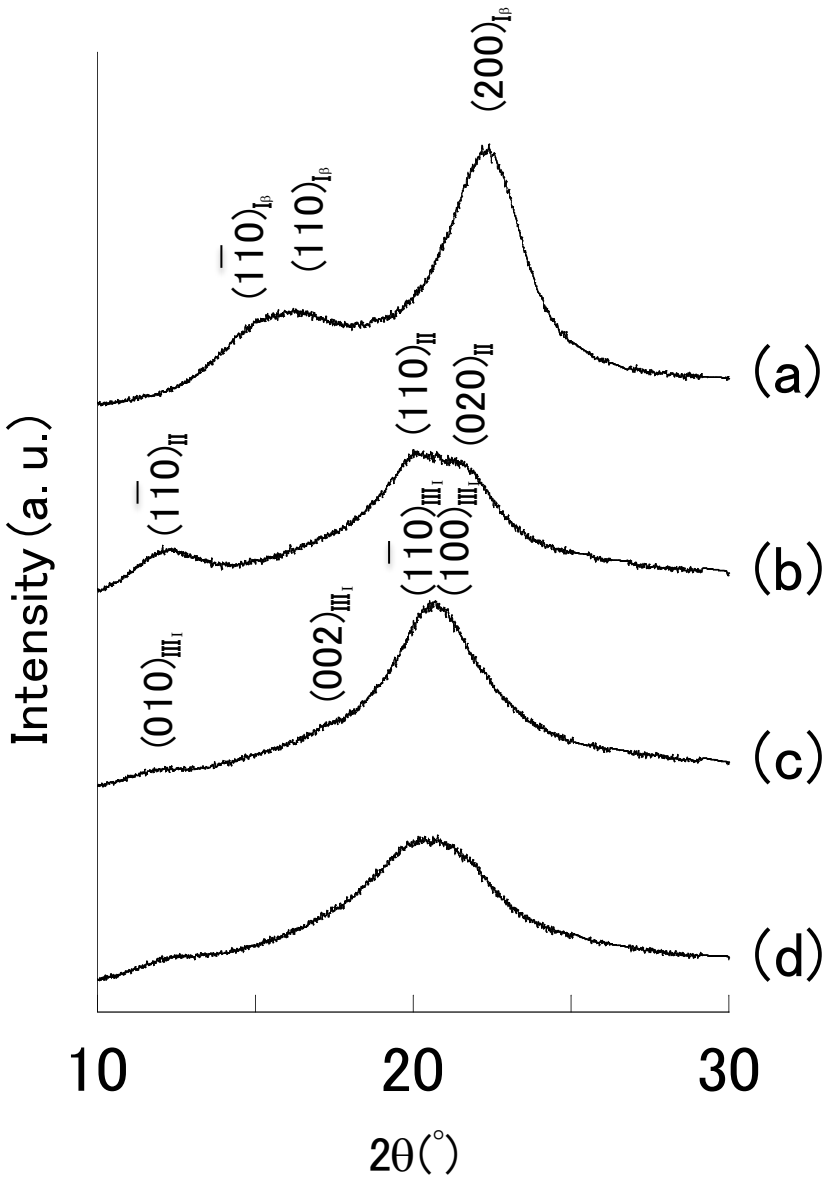
Intensity (a. u.)
(200)Iβ
(1̄10)Iβ
(110)Iβ
(a)
(1̄10)II
(110)II
(020)II
(b)
(010)III1
(002)III1
(1̄10)III1
(100)III1
(c)
(d)
10
20
30
2θ(°)

Figure 2

385

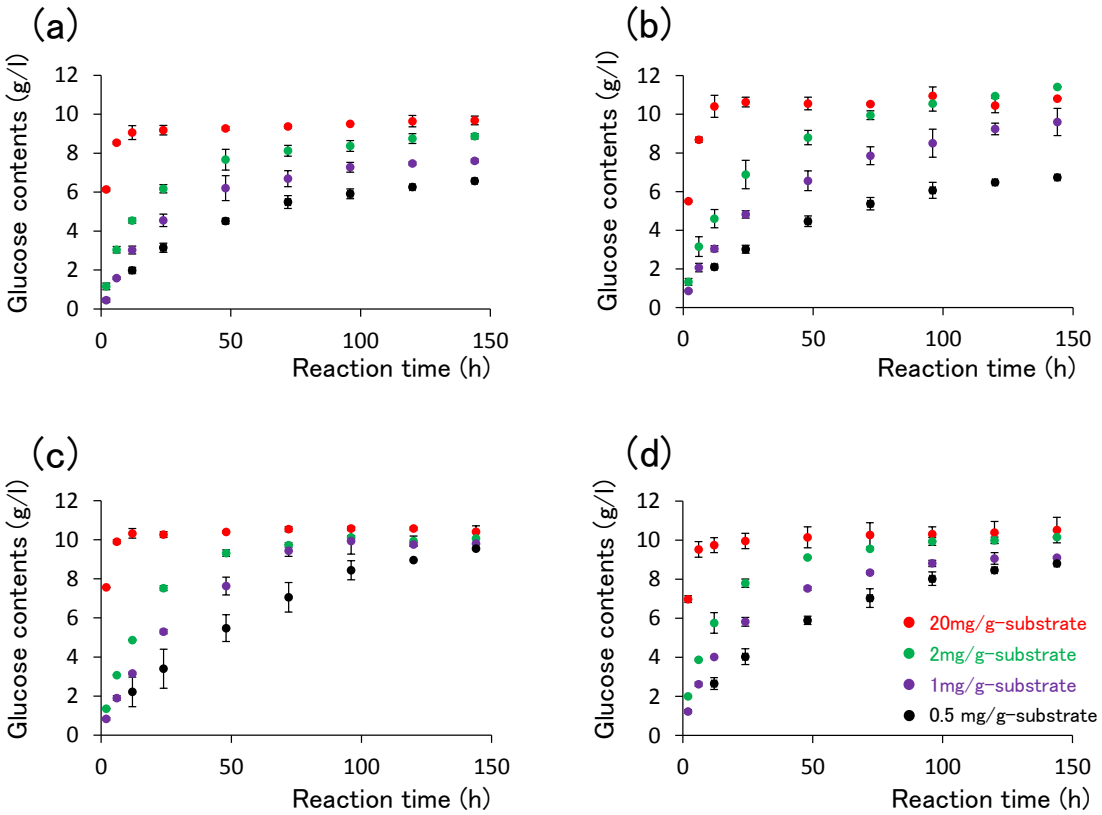

386

387 Figure 3

388

389

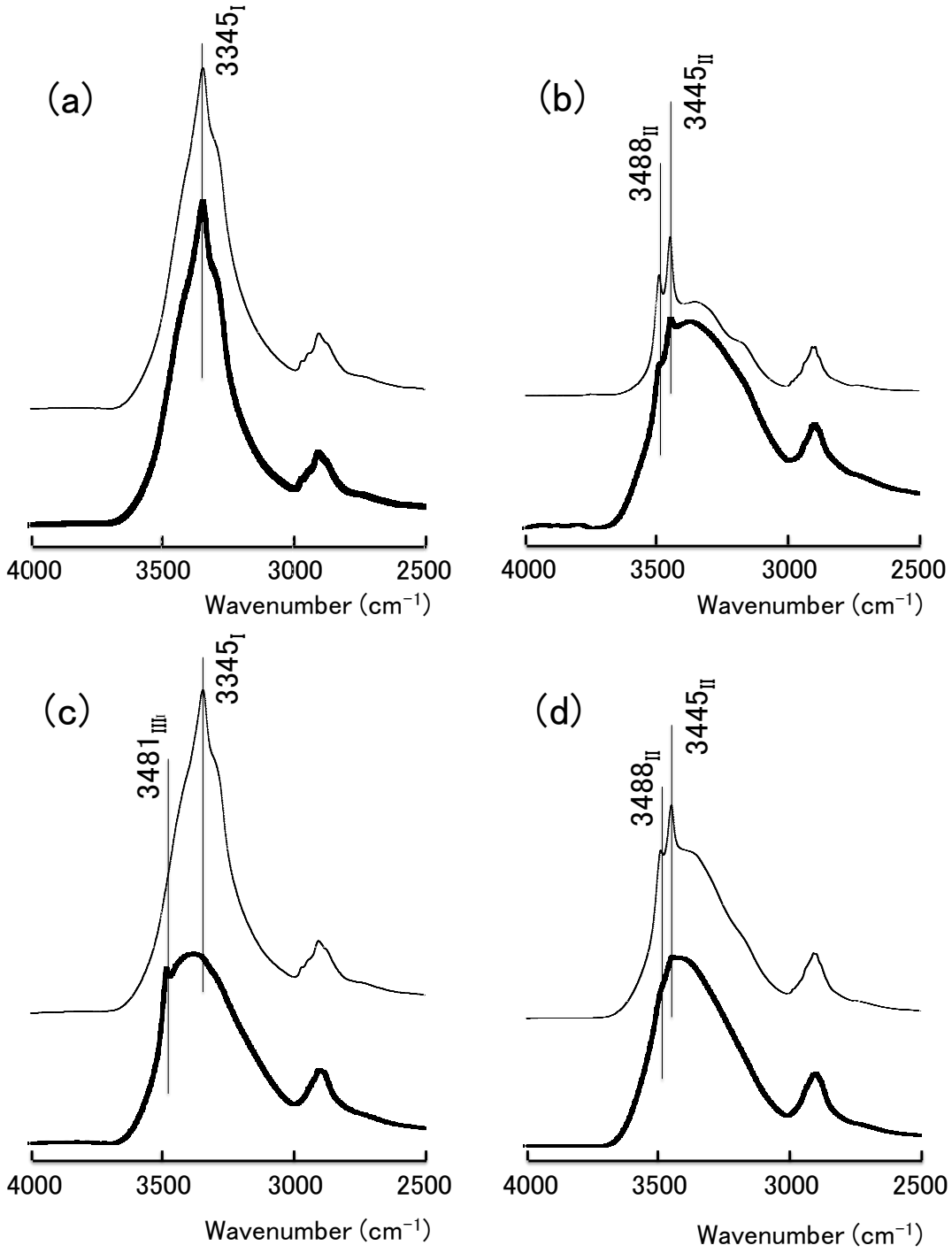

390

391

392 Figure 4

393

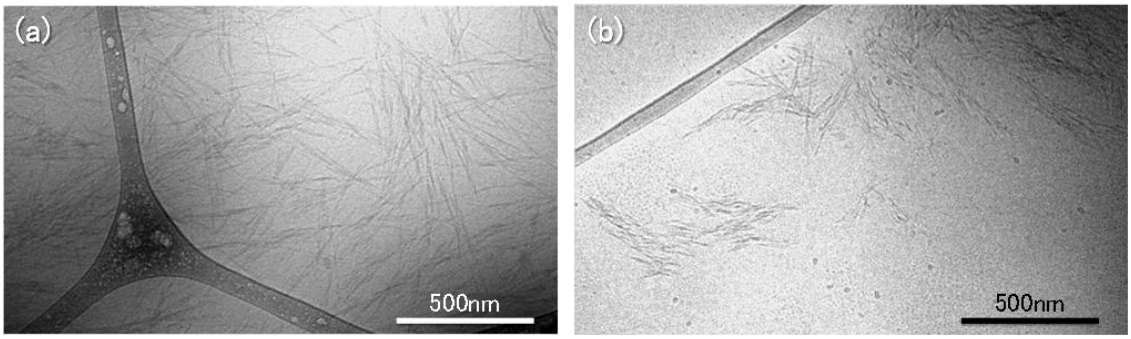

Figure 5

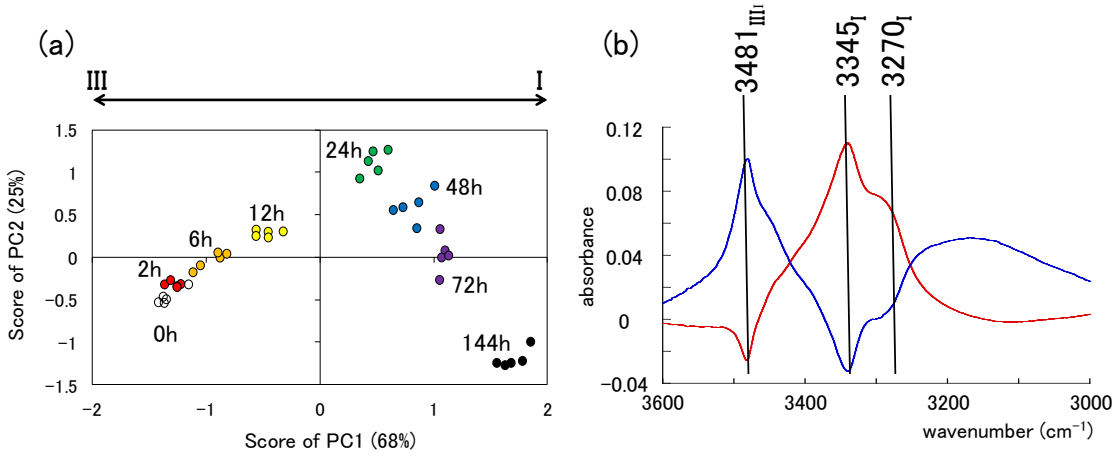

Figure 6

158 Line174 subscript of Miller index indicates crystalline polymorphs; β→cellulose I_{β}, II→cellulose II, III→cellulose III, respcectively.